From multilayers to V1-xWxO2±δ films elaborated by magnetron sputtering for decreasing thermochromic transition temperature

Jean-Louis L Victor, Corinne Marcel, Laurent Sauques, Christine Labrugère, Frederic Amiard, Alain Gibaud, Aline Rougier

▶ **To cite this version:**

Jean-Louis L Victor, Corinne Marcel, Laurent Sauques, Christine Labrugère, Frederic Amiard, et al.. From multilayers to V1-xWxO2±δ films elaborated by magnetron sputtering for decreasing thermochromic transition temperature. Journal of Alloys and Compounds, 2021, 858, 157658 (7 p.). 10.1016/j.jallcom.2020.157658 . hal-02976017

HAL Id: hal-02976017

https://univ-lemans.hal.science/hal-02976017

Submitted on 5 Nov 2020

HAL is a multi-disciplinary open access archive for the deposit and dissemination of scientific research documents, whether they are published or not. The documents may come from teaching and research institutions in France or abroad, or from public or private research centers.

L'archive ouverte pluridisciplinaire **HAL**, est destinée au dépôt et à la diffusion de documents scientifiques de niveau recherche, publiés ou non, émanant des établissements d'enseignement et de recherche français ou étrangers, des laboratoires publics ou privés.

From multilayers to $V_{1-x}W_xO_{2\pm\delta}$ films elaborated by magnetron sputtering for decreasing thermochromic transition temperature

J.L. Victor[a,e], C. Marcel[a], L. Sauques[b], C. Labrugère[c], F. Amiard[d], A. Gibaud[d], A. Rougier[e*]

[a] CEA-DAM, Le Ripault, Monts F-37260, France
[b] Centre d'Expertise Parisien de la Délégation Générale à l'Armement, Paris F-75015, France
[c] CNRS, Univ. Bordeaux, PLACAMAT, UMS 3626 F-33600, Pessac, France
[d] CNRS, Univ. du Mans, IMMM (UMR 6283), Le Mans F-72085, France
[e] CNRS, Univ. Bordeaux, Bordeaux INP, ICMCB (UMR 5026), Pessac F-33600, France
* corresponding author : aline.rougier@icmcb.cnrs.fr

Abstract

W-doped monoclinic vanadium dioxide VO_2(M) thin films with various W contents were successfully deposited by magnetron sputtering method. As-deposited films consisted of multilayers composed of VO_2/W bilayers. Further annealing at 500 °C under Argon for 1 h led to crystallized and homogeneous $V_{1-x}W_xO_{2\pm\delta}$ films. 200 nm films were characterized at room temperature by Rutherford backscattering spectrometry (RBS), X-ray diffraction (XRD) and X-ray photoelectron spectroscopy (XPS). Besides, the films were analyzed by temperature-dependent infrared transmittance in the wavelength region 2-25 µm and the effects of W doping on thermochromic properties of VO_2 were studied. The results show that the transition temperature gradually decreases with increasing W content. A transition temperature of 21 °C with a high infrared transmittance modulation (≈ 68 %) was finally achieved with a W-doping level of 2.7 at.% which may indicate a strong potential for applications in optical devices as functional materials.

Keywords

Magnetron sputtering, multilayers, vanadium dioxide, W doping, thermochromic behavior

1. Introduction

Materials with tunable Metal-Insulator Transition (MIT) are of great interest in various applications such as thermals sensors, electronic switches, adaptive infrared camouflage, smart windows, etc [1, 2, 3]. Among several MIT materials, vanadium dioxide (VO_2) shows a first order reversible transition from a monoclinic structure (M1, P21/c) to a rutile structure (R, P42/mnm) at around 68 °C [4] which is closer to room temperature than any other thermochromic materials.

Above the phase transition temperature, the partially filled 3d// band is localized at the Fermi level giving to VO_2 a metallic behavior. The temperature decrease induces displacement of V^{4+} leading to the splitting of the 3d// band and destabilization of the π band. Thus, all electrons are transferred to the lowest energy 3d// band corresponding to a bandgap of ~0.6 eV opening up between $\pi*$ and the filled part of 3d// band giving to the material a semiconductor state [5]. Thus, the reversible phase transition involves an abrupt change in optical, electronic and structural properties of VO_2. Nevertheless, the variation in these properties as a function temperature induces a thermal hysteresis [6]. A higher thermal activation energy is needed during the heating cycle to transform the low-temperature monoclinic phase VO_2 into the high-temperature rutile state. The nature of the hysteresis curves depends very strongly on the nano- and microcrystalline nature of VO_2 [7]. Several chemical and physical methods have been developed to grow dense and continuous VO_2 based films including CVD, Sol-gel, solutions methods and magnetron sputtering [8, 9, 10]. However, vanadium can form many different oxides when exposed to oxygen (such as V_2O_3, V_4O_7, V_3O_5, V_3O_7, V_2O_5..) [11], so developing an efficient and reproducible technique to form stoichiometric VO_2 thin films is of critical importance for VO_2-based devices.

As mentioned above, the metal-insulator transition of VO_2 occurred at 68 °C which is too high for room temperature applications. One way to reduce the transition temperature is to substitute V^{4+} ions by metal ions with higher valence such as W^{6+}, Nb^{5+}, Mo^{6+} [12, 13, 14, 15]. Among them, W has been considered as one of the most effective ion, lowering the transition temperature (Tc) by 24 °C

per 1 at.% [12] while 7.5 °C per 1 at.% and approximatively 8 °C per 1 at.% have been reported for Nb [13] and Mo [16], respectively.

In this paper, an innovative method for the deposition of W-doped VO_2 thin films by magnetron sputtering is studied. Indeed, multilayers composed of VO_2/W bilayers are first prepared allowing to govern the W content by adjusting the thickness of the W layer. The main advantage of this process as compared to co-sputtering deposition is its repeatability. Indeed, co-sputtering can caused thickness and composition inhomogeneity issues and contamination between the targets. Then, an annealing step at 500 °C under Ar flow is performed to allow both crystallization of VO_2 monoclinic phase and diffusion of W through the VO_2 layers to form homogeneous W-doped VO_2 film. Furthermore, the thermochromic properties of the films have been investigated with optical transmittance in the mid-infrared range.

2. Experimental section

2.1. Preparation of W-doped VO_2 thin films by magnetron sputtering

W-doped VO_2 thin films were prepared from annealing of multilayers composed of VO_2/W bilayers. Layers were deposited on (001) oriented silicon substrate by cylindrical DP650 magnetron sputtering device (ALLIANCE CONCEPT). The Si-(001) substrates were selected for their optical transparency in the infrared range. Pulsed Direct Current Magnetron Sputtering (PDCMS) was used as magnetron supply. The pulse repetition frequency and duration time were 50 kHz and 2 µs. VO_2 layers were deposited from vanadium target of high purity (99.9 %_GENCOA) with 75 mm diameter in an Ar + O_2 environment. During the deposition process, Ar and O_2 gas flow rates were fixed at 60 sccm and 2.4 sccm, respectively for a total sputtering pressure of 1 Pa. A sputtering power of 250 W was used for each VO_2 layer deposition.

W layers were deposited from a 150 mm diameter tungsten target (99.9 %_ALLIANCE CONCEPT) in an Ar discharge with a power supply fixed at 100 W. The Ar flow rate was set to 30 sccm for a total gas pressure maintained at about 0.7 Pa.

Three different multilayers were deposited. The VO_2 and W thicknesses were adjusted in order to obtain multilayers with different (W/V) atomic ratios of 0.8 (Sample A), 1.8 (Sample B), 2.9 (Sample C) respectively (*Table 1)*. To ensure ultra-thin layers of W, a dynamic mode deposition was used. The substrate holder was fixed on a rotating plate during the process. The deposition of W was performed through various stages. Firstly the power supply was applied on the W target to create the discharge while the substrate was positioned at 180 ° from the W target. No deposition occurred during this first step. Then the rotating plate was activated to do a complete rotation allowing the deposition of a very thin film of W when the substrate moved under the W target. The rotation speed was adjusted in respect of the expected thicknesses of W layers.

The W content in the multilayers is determined by $\%_{at}W = n(W)/[n(W) + n(VO_2)]$ but can be approximated for low doping ratio by the following formula :

$$\%_{at}W \approx \frac{n(W)}{n(VO_2)} = \frac{\mu(W) \times [N(W) \times e(W)] \times M(VO_2)}{\mu(VO_2) \times [N(VO_2) \times e(VO_2)] \times M(W)}$$

with
- *n(X) amount of substance (mol)*
- *μ(X) density ($g.cm^{-3}$) [$\mu(VO_2) = 4.57\ g.cm^{-3}$ et $\mu(W) = 19.3\ g.cm^{-3}$)]*
- *M(X) molar mass ($g.mol^{-1}$) [$M(VO_2) = 82.9\ g.cm^{-3}$ et $M(W) = 183.8\ g.cm^{-3}$)]*
- *e(X) thickness of each layer (cm)*
- *N(x) Number of layers*

Equation 1 : Theoretical calculation of the W content

The total thickness of the films was measured with a Veeko Dektak 8 profilometer.

	Sample A	*Sample B*	*Sample C*
VO_2 thickness layer (nm)	25	20	20
Number of VO_2 layers	8	10	10
W thickness layer (nm)	0.10	0.19	0.30
Number of W layers	8	10	10
Theoretical W content (%)	0.8	1.8	2.9
Total thickness expected (nm)	201	202	203
Total thickness measured ± 5 (nm)	203	215	220

Table 1 : Multilayers deposited by PDCMS

An annealing step at 500 °C under Ar flow during 1 hour was then performed to allow the crystallization of VO_2 and diffusion of W through the VO_2 layers. Both heating and cooling rates were adjusted at 2 °C.min^{-1} and the Ar gas flow was fixed at 0.5 L.min^{-1} during the whole process.

2.2. Characterization of the W-doped VO_2 films

The composition and dopant profile were examined by RBS (Rutherford backscattering spectrometry) with 2 MeV He ions at a scattering angle of 170°. Rutherford simulation program (SIMNRA) was used to simulate the RBS patterns.

A ThermoFisher Scientific K-ALPHA spectrometer was used for XPS surface analysis with a monochromatized AlKα source (hν = 1486.6 eV). X-Ray spot size was 400 microns for points acquisition. A pressure of 10^{-7} Pa was reached in the main chamber when transferring the thin layers. The full spectra (0-1100 eV) were obtained with a constant pass energy of 200 eV and high resolution spectra at a constant pass energy of 40 eV. Charge neutralization was applied during analysis. High resolution spectra (i.e. C1s, O1s-V2p, V3p-W4f, N1s, Si2p) were fitted using the AVANTAGE software provided by ThermoFisher Scientific (Scofield sensitivity factors used for quantification).

The structure of the films was identified by Bruker D8 Discover X-ray diffraction at a grazing angle of 2° using CuKα radiation with a wavelength of 0.15405 nm.

The spectral transmittance in the wavelength range of 2.5 µm – 25 µm at normal incidence was measured using Fourier transform infrared spectroscopy (FTIR, Bruker Vertex 70v). A cryostat and liquid nitrogen were used to perform transmittance measurements between -40 and 90 °C. A thermocouple was positioned right next to the films to know the exact value of temperature.

3. Results and discussion

3.1. Composition and dopant profile

Fig.1(a) shows the RBS spectra of the as-deposited films on Si substrate before the annealing step. The W profile is clearly visible for each sample and reveals an inhomogeneous distribution of W in the films (i.e. presence of oscillations/waves) due to the multilayer deposition process. The intensity of vanadium peak is the same for all films, whereas the intensity of tungsten peak differs from one sample to another one meaning a different (W/V) atomic ratio. The intensity decreases from samples

C to A. From simulated spectra (continuous line on *Fig.1*), W content was estimated at 0.7, 1.8 and 2.7 at.% for sample A, B, C respectively. These experimental values are very close to the expected ones determined from the theoretical calculations (*Table 1*). Thus, in the following, the films will be determined by their composition, namely 0.7 % W, 1.8 % W and 2.7 % W.

Fig.1(b) shows the RBS spectra of the films on Si substrate after the annealing treatment. The W profile distribution has become homogeneous revealing the positive impact of the annealing step. Besides, the annealing treatment does not affect W content in the films. Indeed, identical W contents were found after the annealing treatment.

3.2. Structural properties

The XRD patterns of VO_2 and W-doped VO_2 films annealed at 500 °C are shown in *Fig.2*. The presence of the (011), (200), (210), (211) and (022) peaks in the patterns confirms that the films crystallize in the P21/c monoclinic space group. No peaks belonging to W or WO_3 are detected for the W-doped VO_2 films, indicating the effective diffusion of W into the VO_2 layers by annealing and thus the formation of $V_{1-x}W_xO_{2\pm\delta}$ solid solution. In the following, this notation will be used to name the films. There was no quite discernible change in the XRD patterns among $V_{1-x}W_xO_{2\pm\delta}$ thin films except that XRD peak positions slightly shift towards the smaller 2θ angles for the samples with the highest doping contents (as can be clearly seen in the inset of *Fig.2*). The ionic radius of W cation is larger than that of V cation [17]. So when W cations substitute partial V cations in VO_2 lattice, the d-value becomes larger, resulting in the peaks shift to low diffraction angle. This result could further confirm that W was successfully captured into the crystal lattice of VO_2(M). We can also attribute this phenomena to the process of phase transformation from VO_2 (M) to VO_2 (R) at room temperature (RT). The inset of *Fig.*2 shows the possible transformation from (011) VO_2(M) to (110) VO_2(R). This suggests that the coexistence of VO_2 (M) and VO_2 (R) could be stabilized at RT by effectively W doping [18]. The average crystallite size, D (nm), found between 16 and 24 nm were calculated from Debye-Scherrer formula via full-width at half maximum (β) of XRD lines [19]. *Table 2* presents

values of 2θ, d, β and D corresponding to (011) peak of the films. We can observe a decrease of crystallite size with W content. This can be attributed to the structural defects induced by doping which caused a structural disorder in the crystal lattice.

W content (at.%)	*2θ (°)*	*d (Å)*	*β (°)*	*D ± 0.5 (nm)*
0	27.947	3.190	0.343	23.9
0.7	27.924	3.196	0.469	17.5
1.8	27.848	3.201	0.430	19.0
2.7	27.813	3.205	0.511	16.0

Table 2 : XRD analysis of $V_{1-x}W_xO_{2\pm\delta}$ films corresponding to (011) VO_2(M) peak

3.3. Surface analysis

XPS analysis of $V_{1-x}W_xO_{2\pm\delta}$ thin films annealed at 500 °C were carried out to investigate the valence of V and W elements. High-resolution XPS spectra of W-4f core-levels are shown in *Fig.3*. The peaks of W-$4f_{5/2}$ and W-$4f_{7/2}$ are located at 37.2 eV and 35.1 eV for all films which indicates that the oxidation state of W ions in the $V_{1-x}W_xO_{2\pm\delta}$ thin films is +6 [18, 20, 21]. However, these binding energies are slightly higher than for W^{6+} in WO_3 oxide (W-$4f_{5/2}$ ~ 37.6 eV and W-$4f_{7/2}$ ~ 35.5 eV) [22, 23] revealing an interaction between W^{6+} and V^{n+} cations in the $V_{1-x}W_xO_{2\pm\delta}$ thin films. It implies that tungsten atoms are successfully doped into VO_2 films.

Fig.4 shows the high resolution XPS spectra of V-2p core-level. The V-$2p_{3/2}$ peak is well fitted and three different valence forms are observed : V^{5+} ($2p_{3/2}$-517.1 eV), V^{4+} ($2p_{3/2}$-515.8 eV) and V^{3+} ($2p_{3/2}$-514.7 eV) [20]. The observation of V^{5+} is due to highly surface sensitive of XPS analysis. The surface of the samples was exposed to air, which could induce a surface oxidation of VO_2 since V_2O_5 is the most stable phase of vanadium oxide. The presence of V^{3+} valence states indicates a reduction in the oxidation state of V from V^{4+} to V^{3+} for the electronic compensation by the doping of W^{6+} ion. In order to show the influence of W content on valence states of V, the proportion of V^{5+}, V^{4+} and V^{3+} was estimated from fitted curves and gathered in *Table 3*. The increase of V^{3+} ions proportion with the W content confirms that the charge compensation in the $V_{1-x}W_xO_{2\pm\delta}$ films is partially due to V^{3+} valence state.

W content (at.%)	*V^{3+} (%)*	*V^{4+} (%)*	*V^{5+} (%)*
0	0	72.8	27.2
0.7	7.6	61.2	31.2
1.8	8.4	61.8	29.8
2.7	10.1	54.1	35.8

Table 3 : Influence of W content on $V^{3+}/V^{4+}/V^{5+}$ proportions

3.4. Thermochromic properties

The optical transmittance measurements were carried out at normal incidence in the spectral domain ranging from 2.5 µm to 25 µm. Silicon substrate contribution was removed by dividing the transmittance sample signals by the nude silicon transmittance. *Fig.5* shows the optical transmittance spectra at different temperatures for the $V_{1-x}W_xO_{2\pm\delta}$ thin films during heating. Temperatures were chosen for each sample to cover the optical response from the semiconducting state to the metallic state. As expected, the optical transmittance exhibits strong change as the temperature increases, indicating a pronounced thermochromic behaviour. The beginning of the transmittance variation does not occur at the same temperature for all samples and depends strongly on the W content. Indeed, the magnitude of transmittance starts to change at 50 °C for the VO_2 film and 40 °C, 10 °C and -5 °C for films doped at 0.7, 1.8 and 2.7 at.% W respectively. The low temperature spectra for each film exhibit distinct phonon vibration peaks at 16.6 µm and 19.2 µm attributed to the V-O-V octahedral bending modes in the semi-conductive state [24]. At low temperature, the electrons involved in the V^{4+}–V^{4+} bonds are localized, whilst at high temperature these electrons are delocalized due to the metal state of the material. This plasma of free carriers involves a screening effect for the incident photons. Consequently, no vibrational absorption bands are observed and the transmittance drastically decreases due to an increase in reflectivity.

To determine the thermochromic properties of $V_{1-x}W_xO_{2\pm\delta}$ films, measurements were also performed upon a cooling phase to generate a complete cycle. *Fig.6.a* shows a thermal hysteresis loop of the intrinsic transmittance−temperature plot at a fixed wavelength of 10 µm for the $V_{1-x}W_xO_{2\pm\delta}$ films. The switching temperature values during heating [Tc(H)] and cooling [Tc(C)] were deducted from

the half-value width of each curve and the average temperature of commutation (Tc) representative of a thermochromic behaviour was defined as Tc = [Tc(H) + Tc(C)]/2. The optical performance of the films was expressed in *Table.4* by calculating the infrared transmittance modulation ΔTr (%) from the difference between the lowest and the highest temperature states. W-doping dramatically reduces the transition temperature with a decrease from 63 °C to 21 °C as W content increases from 0 to 2.7 at.%. Each tungsten ion into the VO_2 lattice breaks up a V^{4+}–V^{4+} homopolar bond. For charge compensation, two W-3d electrons are transferred to a nearest neighbour vanadium ion, thus forming a V^{3+}-W^{6+} and a V^{3+}-V^{4+} pair [25]. The loss of homopolar V^{4+}-V^{4+} bonding destabilizes the semiconducting phase and lowers the metal-semiconductor transition temperature. The dependence of the phase transition temperature on the tungsten concentration is linear (*Fig.6.b*). The drop of transition temperature is estimated to be about 15 °C per 1 at.% of W doping. This decreasing efficiency is less than that described in other reports which mention more than 20 °C per 1 at.% W [12, 25]. It is likely that the tungsten ions are not completely incorporated into VO_2 crystallographic structure. However, according to the XRD patterns shown in *Fig. 2*, no peaks ascribed to compounds containing W were revealed. Thus, we assume that the residual W remains as an amorphous phase.

For low W content (0.7 at.%), the decrease in Tc is noticeably associated with no modification of the amplitude modulation of the transmittance (close to 90 %). For higher W content, the lowering of Tc is accompanied by a pronounced degradation of the optical performances. Indeed, as the doping level increases, the transmittance at low temperature decreases progressively, whilst at high temperature, the samples exhibit the same level for low transmittance state regardless of their tungsten content.

Next, we will focus on the hysteresis behaviour. The hysteresis loop width gradually narrows from 12 °C for the VO_2 film to 5 °C for the film doped with 2.7 at.% W. It illustrates that the W dopant not only reduces the transition temperature, but also narrows the hysteresis loops width. Structural defects induced by W doping play a role as nucleation sites of the phase transition [26]. Therefore, the activation energy of the phase transition would be reduced causing a decrease in hysteresis width. A

VO_2 thin film doped at a theoretical value of 3.6 at.% W was also performed and allowed a decrease of Tc down to 9 °C.

W content (at.%)	*Tc(H) (°C)*	*Tc(C) (°C)*	*ΔTc (°C)*	*Tc (°C)*	*ΔTr (%)*
0	69	57	12	63	89.5
0.7	51	43	8	47	91.4
1.8	36	32	4	34	80.6
2.7	18.5	23.5	5	21	68.4

Table 4: Thermochromic properties of $V_{1-x}W_xO_{2\pm\delta}$ thin films deduced from hysteresis loops

4. Conclusion

An innovative magnetron sputtering method was developed for the preparation of $V_{1-x}W_xO_{2\pm\delta}$ thin films. Multilayers composed of VO_2/W layers were deposited on silicon substrate and annealed at 500 °C under argon atmosphere for 1 h. The as-prepared $V_{1-x}W_xO_{2\pm\delta}$ films were characterized by RBS, XRD, XPS, and temperature dependence of the transmittance in the mid-infrared range. The results show that W^{6+} ions are successfully doped into the crystal lattice of VO_2(M). Temperature dependent optical transmittance measurements reveal a large switching efficiency for the four $V_{1-x}W_xO_{2\pm\delta}$ films. Four transition temperatures of 63 °C, 47 °C, 34 °C and 21 °C were achieved with W-doping levels of 0, 0.7, 1.8 and 2.7 at.% respectively. These very good thermochromic properties can be used for the development of smart coating and optical devices based on thermochromic switching behaviour.

References

[1] C. Napierala, M. Edely, P. Laffez and L. Sauques, "Thermo-optical effect of $Nd_{0.3}Sm_{0.7}NiO_3$ ceramic in the infrared range," *Optical Materials 31,* pp. 1498-1501, 2009.

[2] J. Mizsei, J. Lappalainen, L. Pohl "Active thermal-electronic devices based on heat-sensitive metal-insulator-transition resistor elements," *Sensors and Actuators A 267,* pp. 14-20, 2017.

[3] S. Chen, Z. Wang, H. Ren, Y. Chen, W. Yan, C. Wang, B. Li, J. Jiang and C. Zou, "Gate-controlled VO_2 phase transition for high-performance smart windows," *Science Advances 5,* pp. 1-8, 2019.

[4] Y. D. Ji, T. S. Pan, Z. Bi, W. Z. Liang, Y. Zhang, H. Z. Zeng, Q. Y. Wen, H. W. Zhang, C. L. Chen, Q. X. Jia and Y. Lin, "Epitaxial growth and metal-insulator transition of vanadium oxide thin films with controllable phases," *Applied Physics Letters 101,* pp. 1-5, 2012.

[5] S. Lee, C. Sohn, D. Lee, J. Nichols, D. Lee, S. S. A. Seo, J. W. Freeland, T. W. Noh and H. N. Lee, "Electronic structure and insulating gap in epitaxial VO_2 polymorphs," *APL Materials 3 (026101),* pp. 1-7, 2015.

[6] K. Miyazaki, K. Shibuya, M. Suzuki, H. Wado and A. Sawa, "Correlation between thermal hysteresis width and broadening of metal–insulator transition in Cr- and Nb-doped VO_2 films," *Japanese Journal of Applied Physics 53 (071102),* pp. 1-5, 2014 .

[7] X. Xu, X. He, H. Wang, Q. Gu, S. Shi, H. Xing, C. Wang, J. Zhang, X. Chen and J. Chu, "The extremely narrow hysteresis width of phase transition in nanocrystalline VO_2 thin films with the flake grain structures," *Applied Surface Science 261 ,* pp. 83-87, 2012.

[8] J. Fortier, B. Baloukas, O. Zabeida, J. Klemberg-Sapieha and L. Martinu, "Thermochromic VO_2 thin films deposited by HiPIMS," *Solar Energy Materials & Solar Cells 125,* pp. 291-296, 2014.

[9] F. Guinneton, L. Sauques, J.-C. Valmalette, F. Cros and J.-R. Gavarri, "Optimized infrared switching properties in thermochromic vanadium dioxide thin films: role of deposition process and microstructure," *Thin Solid Films 446,* pp. 287-295, 2004.

[10] A. García-Wong, D. Pilloud, S. Bruyère, S. Mathieu, S. Migot, J.F. Pierson and F. Capon, "Oxidation of sputter-deposited vanadium nitride as a new precursor to achieve thermochromic VO_2 thin films," *Solar Energy Materials and Solar Cells 210 (110474),* pp. 1-7, 2020.

[11] H. Katzke, P. Tolédano and W. Depmeier, "Theory of morphotropic transformations in vanadium oxides," *Physical review B 68 ,* 2003.

[12] W. Burkhardt, T. Christmann, B. Meyer, W. Niessner, D. Schalch and A. Scharmann, "W- and F-doped VO_2 films studied by photoelectron spectrometry," *Thin Solid Films 345,* pp. 229-235, 1999.

[13] C. Piccirillo, R. Binions and I. Parkin, "Nb-Doped VO_2 Thin Films Prepared by Aerosol-Assisted Chemical Vapour Deposition," *European Journal of Inorganic Chemistry 25 ,* pp. 4050 - 4055 , 2007.

[14] S. Guan, M. Souquet-Basiège, O. Toulemonde, D. Denux, N. Penin, M. Gaudon and A. Rougier, "Toward Room-Temperature Thermochromism of VO_2 by Nb Doping : Magnetic Investigations," *Chemistry of Materials 31,* pp. 9819-9830, 2019.

[15] G. Khan, K. Asokan and B. Ahma, "Room temperature tunability of Mo-doped VO_2 nanofilms across semiconductor to metal phase transition," *Thin Solid Films 625 ,* pp. 155-162, 2017.

[16] L. Mai, B. Hu, T. Hu, W. Chen and E. Gu, "Electrical property of Mo-doped VO_2 nanowire array film by melting-quenching sol-gel method," *Journal of Physical Chemistry B 110,* pp. 19083-19086, 2006.

[17] R. D. Shannon, "Revised effective ionic radii and systematic studies of interatomic distances in halides and chalcogenides," *Acta Crystallographica A. 32 (5),* pp. 751-767, 1976.

[18] S. Dou, W. Zhang, Y. Wang, Y. Tian, Y. Wang, X. Zhang, L. Zhang, L. Wang, J. Zhao and Y. Li, "A facile method for the preparation of W-doped VO_2 films with lowered phase transition temperature, narrowed hysteresis loops and excellent cycle stability," *Materials Chemistry and Physics 215*, pp. 91-98, 2018.

[19] Y. Cheng, X. Zhang, C. Fang, J. Chen, J. Su, Z. Wang and D. L. G. Sun, "Synthesis, structure and properties of printable W-doped thermochromic," *Ceramics International 44 (16)*, pp. 20084-20092, 2018.

[20] S. Chen, H. Lu, S. Brahma and J. Huang, "Effects of annealing on thermochromic properties of W-doped vanadium dioxide thin films deposited by electron beam evaporation," *Thin Solid Films 644*, pp. 52-56, 2017.

[21] S. Liang, Q. Shi, H. Zhu, B. Peng and W. Huang, "One-Step Hydrothermal Synthesis of W-Doped VO_2 (M) Nanorods with a Tunable Phase-Transition Temperature for Infrared Smart Windows," *ACS Omega (1)*, pp. 1139-1148, 2016.

[22] T. H. Fleisch and G. J. Mains, "An XPS study of the UV reduction and photochromism of MoO_3 and WO_3," *Journal of Chemical Physics 76* , pp. 780-786, 1982.

[23] X. Zheng, "The influence of ion implantation-induced oxygen vacancy on electrical conductivity of WO_3 thin films," *Vacuum 165* , pp. 46-50, 2019.

[24] X. Wu, Z. Wu, C. Ji, H. Feng, X. Ma, Y. Su, Y. Zhou, J. Wang and Y. Jiang, "Influence of infrared optical properties by transformation of the crystal structure in Al-doped vanadium dioxide films," *Optical Materials Express 6 (11)*, pp. 3500-3506, 2016.

[25] C. Tang, P. Georgopoulos, M. Fine, J. Cohen, M. Nygren, G. Knapp and A. Aldred, "Local atomic and electronic arrangements in $W_xV_{1-x}O_2$," *Physical Review B 31 (2)*, pp. 1000-1011, 1985.

[26] R. Lopez, T. E. Haynes, L. A. Boatner, L. C. Feldman and R. F. Haglund, "Size effects in the structural phase transition of VO_2 nanoparticles," *Physical Review B 65 (224113)*, pp. 1-5, 2002.

[27] P. Jin, S. Nakao and S. Tanemura, "Tungsten doping into vanadium dioxide thermochromic films by high-energy ion implantation and thermal annealing," *Thin Solid Films 324* , pp. 151-158, 1998.

Graphical abstract

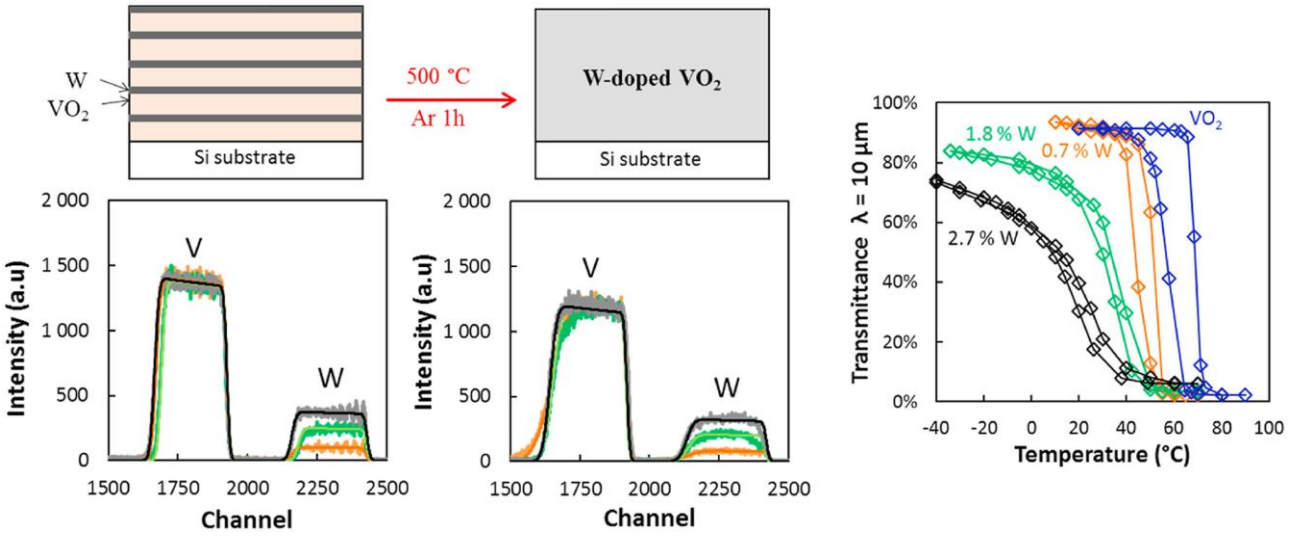

Fig. 1. RBS spectra of the W-doped VO_2 thin films on Si substrate before thermal annealing (a) and after thermal annealing at 500 °C in Ar for 1h (b).

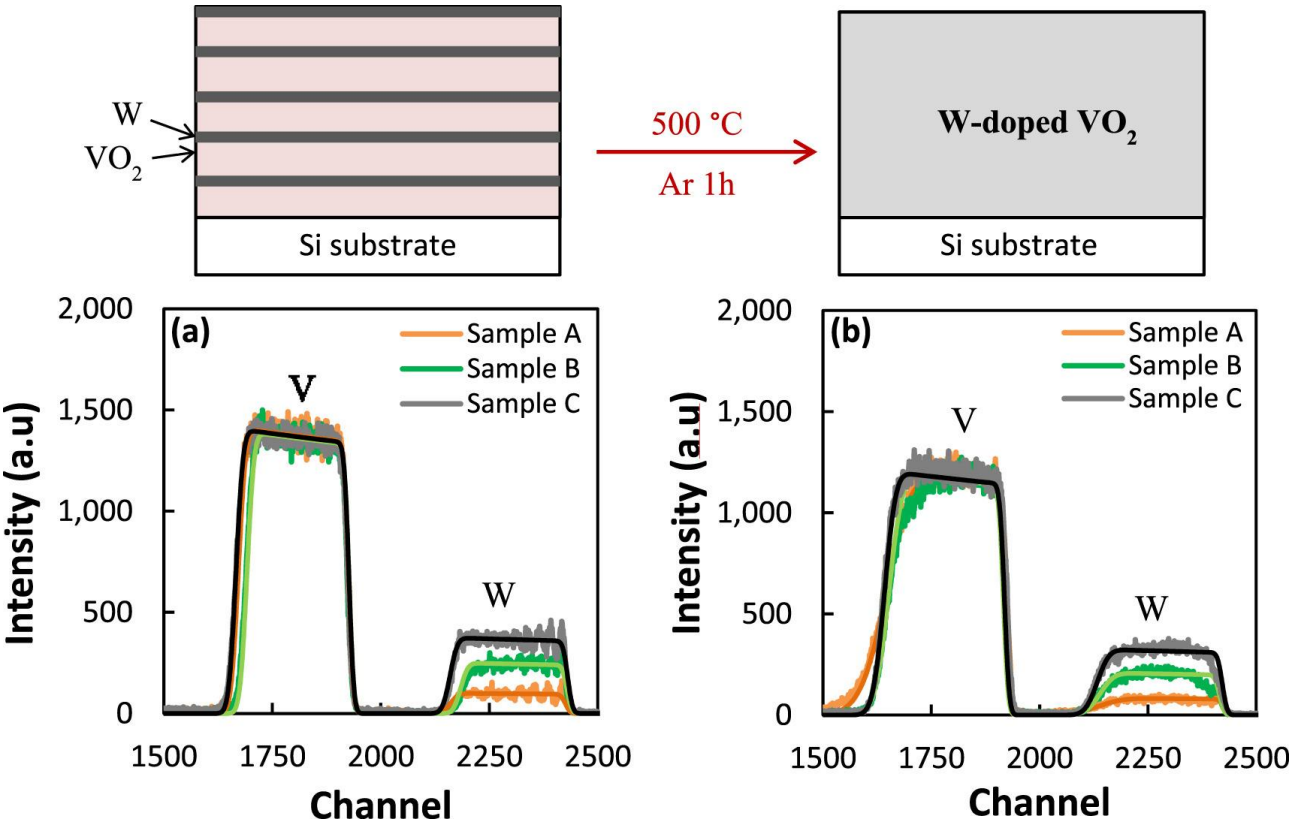

Fig. 2. X-ray Diffraction pattern from θ-2θ scans of $V_{1-x}W_xO_{2\pm\delta}$ thin films deposited by PDCMS and magnification of the 27–29 2θ region corresponding to the VO_2(M) (O11) and VO_2(R) (110), * impurity phase tentatively assigned as V_6O_{13}.

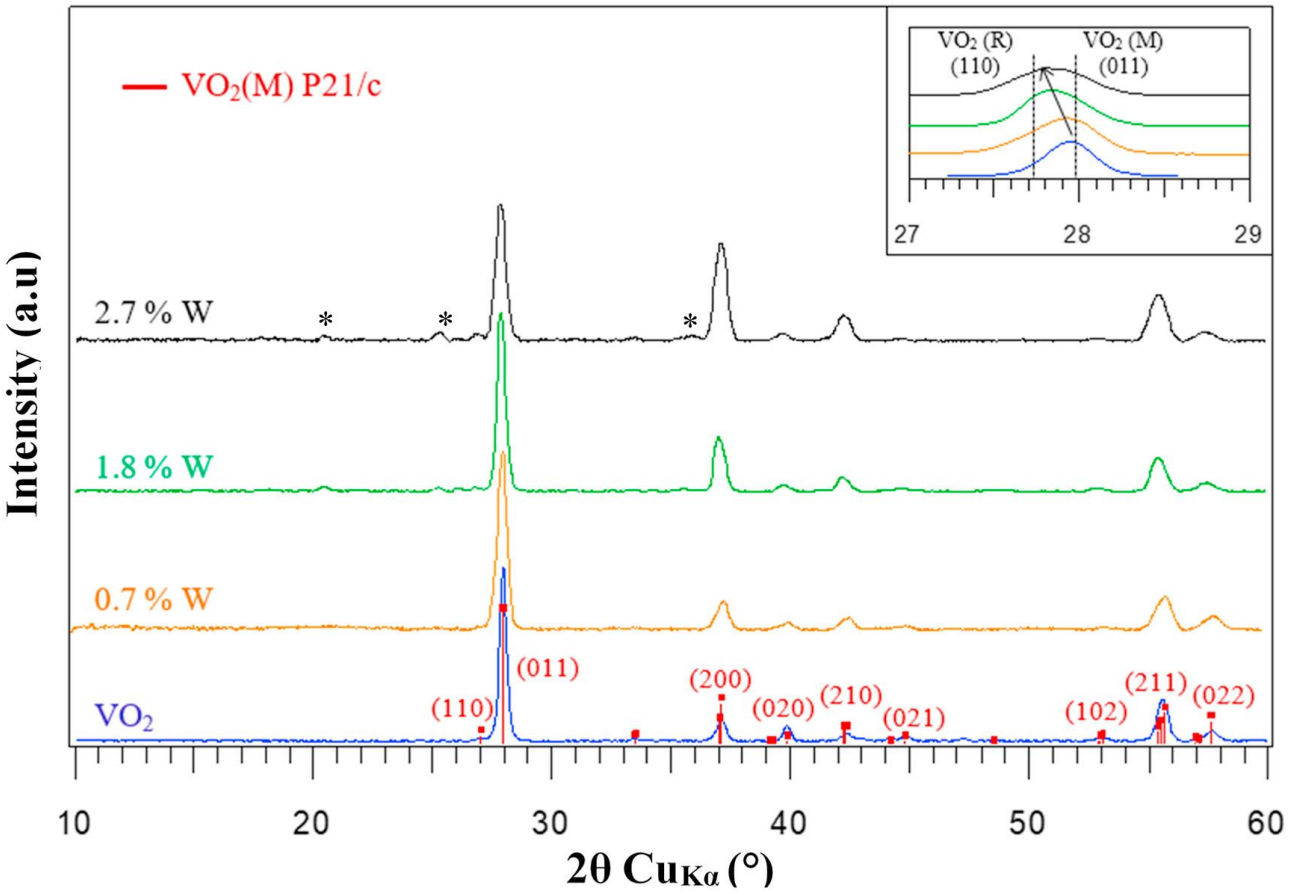

Fig. 3. The core level spectra of W_{4f} of 0.7% W (a) 1.8% W (b) and 2.7% W (c) in $V_{1-x}W_xO_{2\pm\delta}$ films.

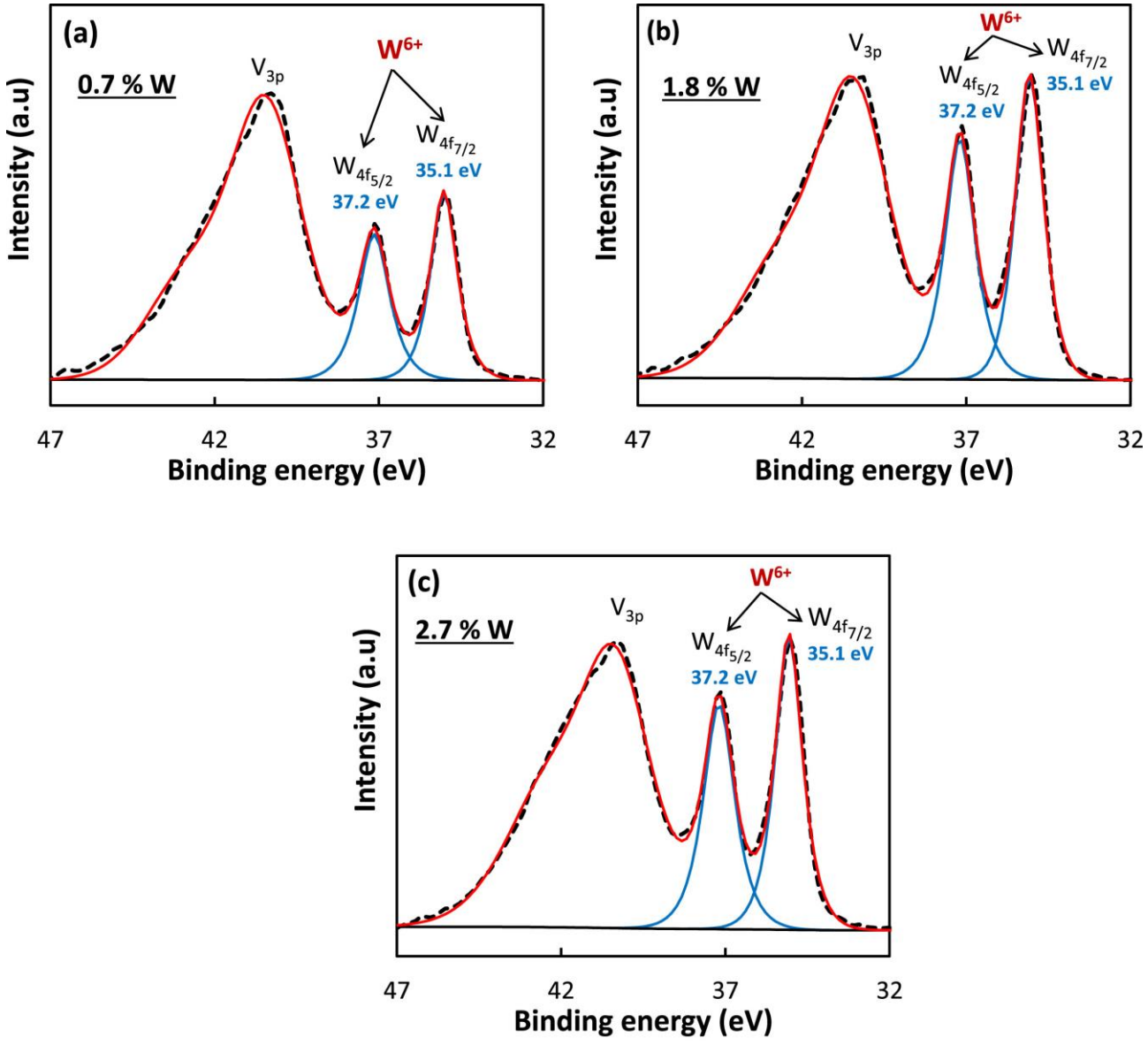

Fig. 4. The core level spectra of V_{2p} of VO_2 (a) 0.7% W (b) 1.8% W (c) and 2.7% W (d) in $V_{1-x}W_xO_{2\pm\delta}$ films.

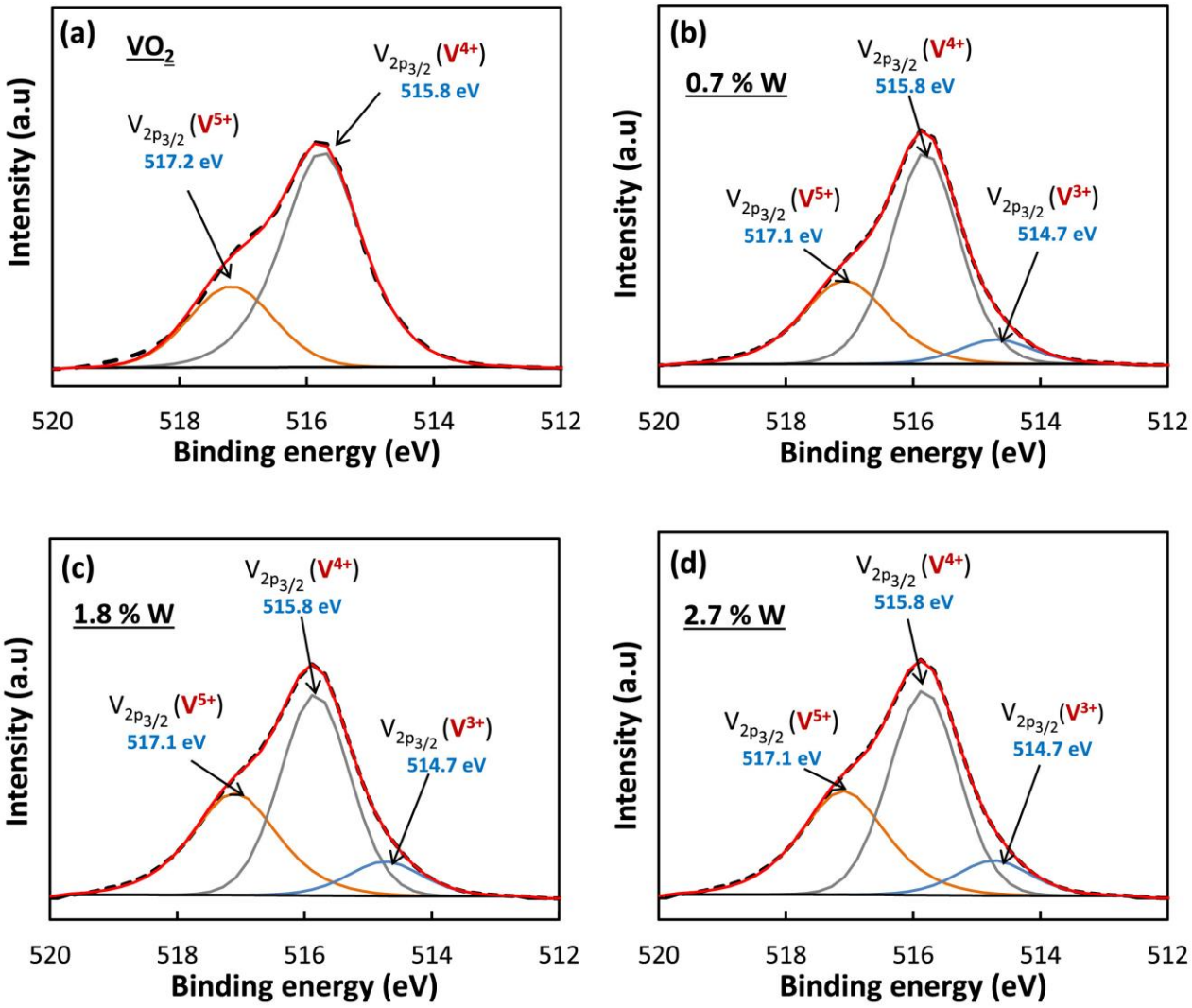

Fig. 5. Variable temperature infrared transmittance spectra of VO_2 (a) 0.7% W (b), 1.8% W (c) and 2.7% W (d) during the heating phase. Film thickness is roughly equal to 200 nm.

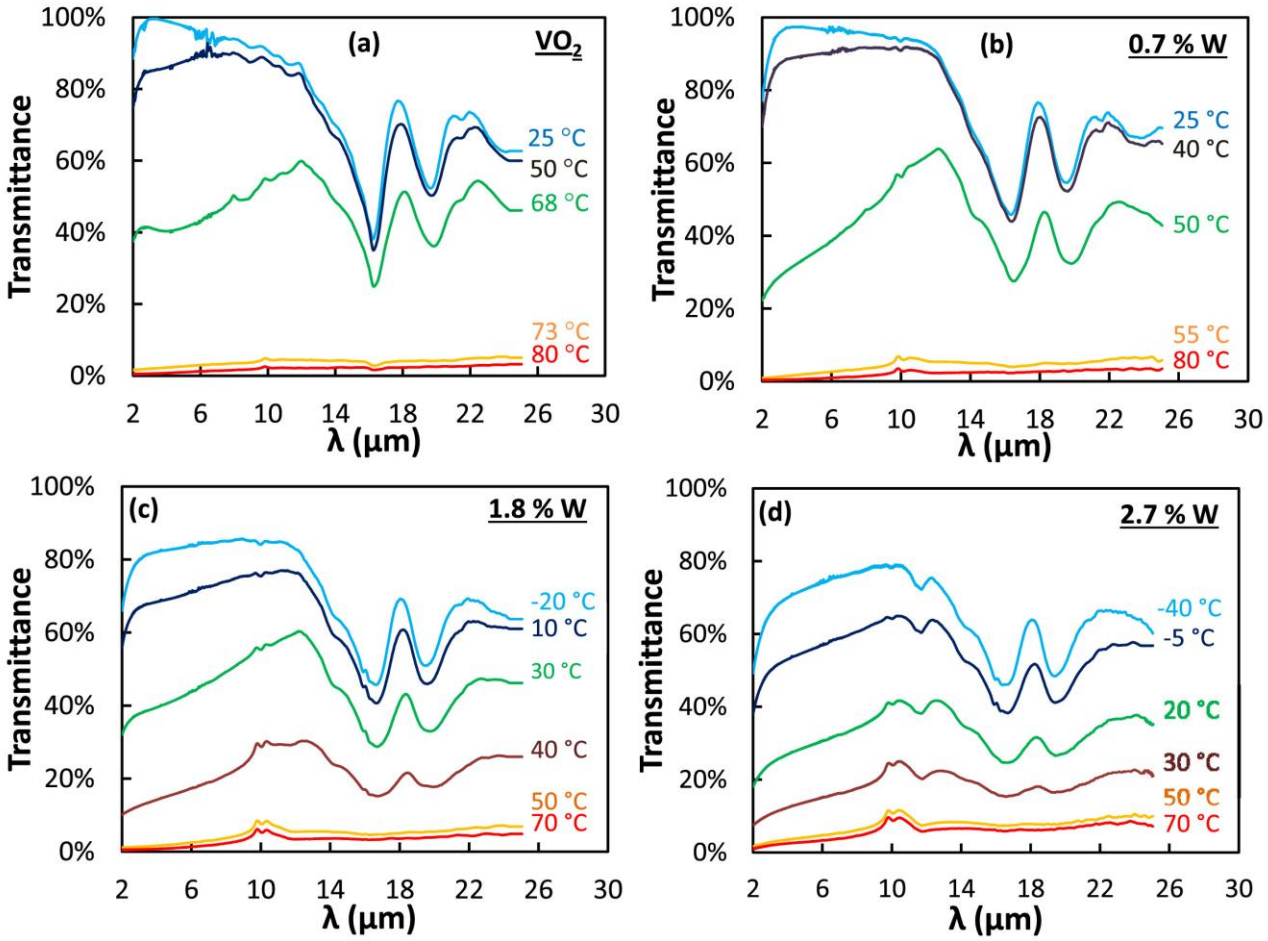

Fig. 6. Transmittance values of 200 nm $V_{1-x}W_xO_{2\pm\delta}$ thin films at 10 µm (a) and relationship between Tc and W concentration (b).